Geologica Acta, Vol.16, Nº 3, September 2018, 237-255
DOI: 10.1344/GeologicaActa2018.16.3.1

geologica acta

Petrography and geochemistry of late- to post-Variscan vaugnerite series rocks and calc-alkaline lamprophyres within a cordierite-bearing monzogranite (the Sierra Bermeja Pluton, southern Iberian Massif)

J. ERRANDONEA-MARTIN[1] F. SARRIONANDIA[2] M. CARRACEDO-SÁNCHEZ[1] J.I. GIL IBARGUCHI[1] L. EGUÍLUZ[2]

[1]Department of Mineralogy and Petrology, Faculty of Science and Technology, University of the Basque Country (UPV/EHU)
Sarriena n/n, 48940 Leioa, Spain

[2]Department of Geodynamics, Faculty of Pharmacy, University of the Basque Country (UPV/EHU)
Paseo de la Universidad 7, 01006 Vitoria-Gasteiz, Spain

ABSTRACT

The Sierra Bermeja Pluton (southern Central Iberian Zone, Iberian Massif) is a late-Variscan intrusive constituted by cordierite-bearing peraluminous monzogranites. Detailed field mapping has allowed to disclose the presence of several NE–SW trending longitudinal composite bodies, formed by either aphanitic or phaneritic mesocratic rocks. According to their petrography and geochemistry these rocks are categorised as calc-alkaline lamprophyres and vaugnerite series rocks. Their primary mineralogy is characterised by variable amounts of plagioclase, amphibole, clinopyroxene, biotite, K-feldspar, quartz and apatite. Broadly, they show low SiO_2 content (49–56wt.%), and high $MgO+FeO_t$ (10–17wt.%), K_2O (3–5wt.%), Ba (963–2095ppm), Sr (401–1149ppm) and Cr (87–330ppm) contents. Field scale observations suggest that vaugneritic rocks and lamprophyres would constitute two independent magma pulses. Vaugneritic dioritoids intruded as syn-plutonic dykes, whereas lamprophyres were emplaced after the almost complete consolidation of the host monzogranites. In this way, vaugnerite series rocks would be an evidence for the contemporaneity of crustal- and mantle-melting processes during a late-Variscan stage, while lamprophyres would represent the ending of this stage.

KEYWORDS **Calc-alkaline lamprophyre. Vaugnerite series. Redwitzite. Cordierite-bearing granite. Iberian Massif.**

INTRODUCTION

Mg-rich ultrapotassic igneous rocks are generally related to volcanic and hypabyssal settings and, among them, lamprophyres are some of the most representative, which usually form subvolcanic dykes, sills, plugs or stocks (Rock, 1991). Calc-alkaline lamprophyres (minettes, kersantites, spessartites and vogesites) constitute a group of rocks enriched in volatiles, Large Ion Lithophile Elements (LILE), alkaline earth and some transition metals (Rock, 1991). Plutonic equivalents of these calc-alkaline types are found across the Variscan Orogeny being referred to with local names such as 'durbachites' (Sauer, 1893), 'vaugnerites' (Fournet, 1837) and 'redwitzites' (Willmann, 1920). Nevertheless, in orogenic areas elsewhere these rocks are known as 'appinites', 'high Sr-Ba granitoids' and 'sanukitoids' (*e.g.* von Raumer *et al.*, 2014 and references therein; Moyen *et al.*, 2017 and references therein).

Traditionally, durbachites, vaugnerites and redwitzites are encompassed in the 'vaugnerite series' and although they share several characteristics, they also display a number of differences as pointed out by Rock (1991) and Sabatier (1991), for instance. Fournet (1837), Michon (1987) and Sabatier (1991) coined the term 'vaugnerite' for a kind of mica-rich diorite composed by biotite, amphibole and plagioclase, with quartz, K-feldspar and abundant accessory apatite. Vaugnerites are basic to intermediate (SiO_2=45–60wt.%), metaluminous rocks with high-K to shoshonitic affinity, characterised by their relatively high FeO_t+MgO values (10–24wt.%) and marked enrichments in both compatible (Mg, Fe, Ni, Cr) and incompatible (K, Rb, Ba, Sr) elements, standing out in particular the high contents in Ba (1000–3000ppm), Sr (500–1000ppm) and Cr (100–600ppm).

Rocks of vaugneritic affinity (referred to with the above mentioned local names) have been described particularly in areas in central Europe (Janoušek *et al.*, 1995; Holub, 1997; Siebel *et al.*, 2003; Buda and Dobosi, 2004; Kováříková *et al.*, 2007; Buzzi *et al.*, 2010) and the Massif Central (Sabatier, 1980, 1991; Montel and Weisbrod, 1986; Michon, 1987; Montel, 1988; Galán *et al.*, 1997). Within the Iberian Massif, such type of rocks have also been identified in the following areas: i) the western areas of Galicia (Gil Ibarguchi, 1980, 1981; Gil Ibarguchi *et al.*, 1984; Gallastegui, 2005); ii) North of Portugal (Dias and Leterrier, 1994; Dias *et al.*, 2002); iii) the Tormes Dome (López Plaza *et al.*, 1999; López-Moro and López-Plaza, 2004; López-Moro *et al.*, 2017); iv) the Toledo Anatectic Complex (Barbero *et al.*, 1990; Barbero, 1992; Bea, 2004; Bea *et al.*, 2006) and v) the Ávila Batholith (Scarrow *et al.*, 2009).

Currently, vaugnerites are a focus of discussion in terms of their geodynamic significance, relative to their emplacement time during the Variscan orogenesis, and the implication of mantle sources in their genesis (*e.g.* von Raumer *et al.*, 2014; Couzinié *et al.*, 2014, 2015, 2016; Laurent *et al.*, 2015; Kubínová *et al.*, 2017, and references therein; Moyen *et al.*, 2017). Vaugneritic magmas seem to derive from a heterogeneous metasomatised mantle, being emplaced during orogenic late- to post-collisional extensional stages (Holub, 1997; Janoušek and Holub, 2007; Solgadi *et al.*, 2007; Scarrow *et al.*, 2009; von Raumer *et al.*, 2014; Couzinié *et al.*, 2016). As for the emplacement timing of the lamprophyres, and thus, their geodynamic significance, this is more debatable since they could represent a late-collisional transtensional stage (*e.g.* Scarrow *et al.*, 2011), or an anorogenic passive rifting stage (*e.g.* Orejana *et al.*, 2008). Despite this unresolved matter, it seems that at least in the case of the calc-alkaline lamprophyres, which would be derived (as the vaugnerites) from a metasomatised mantle source, their emplacement is related to the late-orogenic stages of the Variscan Orogeny (Turpin *et al.*, 1988).

In the Iberian Massif, lamprophyres, vaugnerites and late-orogenic granitoids occur spatially related. Nevertheless, the linkage between the mantle-derived magmas and the host granitoids is controversial in view of the currently most followed petrogenetic models. Thus, for some authors mantle-derived magmas (vaugnerites and appinites) are coeval or slightly older than crustal granitoids and provided heat supply, albeit not enough for the generalized granitoid formation, hence, implying a totally independent genesis (Gil Ibarguchi *et al.*, 1984; Barbero *et al.*, 1990; Bea *et al.*, 1999; Gallastegui, 2005; Scarrow *et al.*, 2009; López-Moro *et al.*, 2017). Alternatively, mantle-derived magmas (gabbros and vaugnerites) and granitoids would be coeval and, besides heat supply, the mafic magmas would be involved (by mixing and/or hybridisation) in the genesis of S-type granitoids (Castro *et al.*, 1999; Alonso Olazabal, 1999; Dias *et al.*, 2002; Carracedo *et al.*, 2009). Other mantle-derived magmas, represented by alkaline lamprophyres, were emplaced clearly after the granitoids in a late- to post-collisional stage (Bea *et al.*, 1999; Orejana *et al.*, 2008; Scarrow *et al.*, 2011).

Whatever the case, the scarcity of mantle-derived rocks in the Iberian Massif (*e.g.* Villaseca *et al.*, 1998; Bea *et al.*, 1999) compared with the huge volume of spatially related granitoids is an open question and calls for more detailed studies of these rocks. In this respect, besides the aforementioned controversy in terms of their geodynamic emplacement setting and their relation to host granitoids, the varied nomenclature of these rocks also calls for a more rigorous classification (*e.g.* Sabatier, 1991; Scarrow *et al.*, 2008). In this contribution we present new petrographic and geochemical (mineral and whole-rock) data of calc-alkaline lamprophyres and intermediate rocks of the vaugnerites series emplaced into the late- to post-Variscan peraluminous Sierra Bermeja Pluton (southern Iberian Massif). We report evidences of the existence of both rock types there and discuss how they compare to similar rocks elsewhere in the Iberian Massif. Furthermore, the emplacement relationships between the studied calc-alkaline lamprophyres and vaugnerite series rocks with the host cordierite-bearing monzogranites, in the frame of the late- to post-Variscan geodynamic evolution, are examined.

GEOLOGICAL SETTING

The Sierra Bermeja Pluton is located 20km to the NE of Mérida (Spain), at the border of the Cáceres and Badajoz provinces, forming an intrusion of ≈60km^2 (Fig. 1A, B).

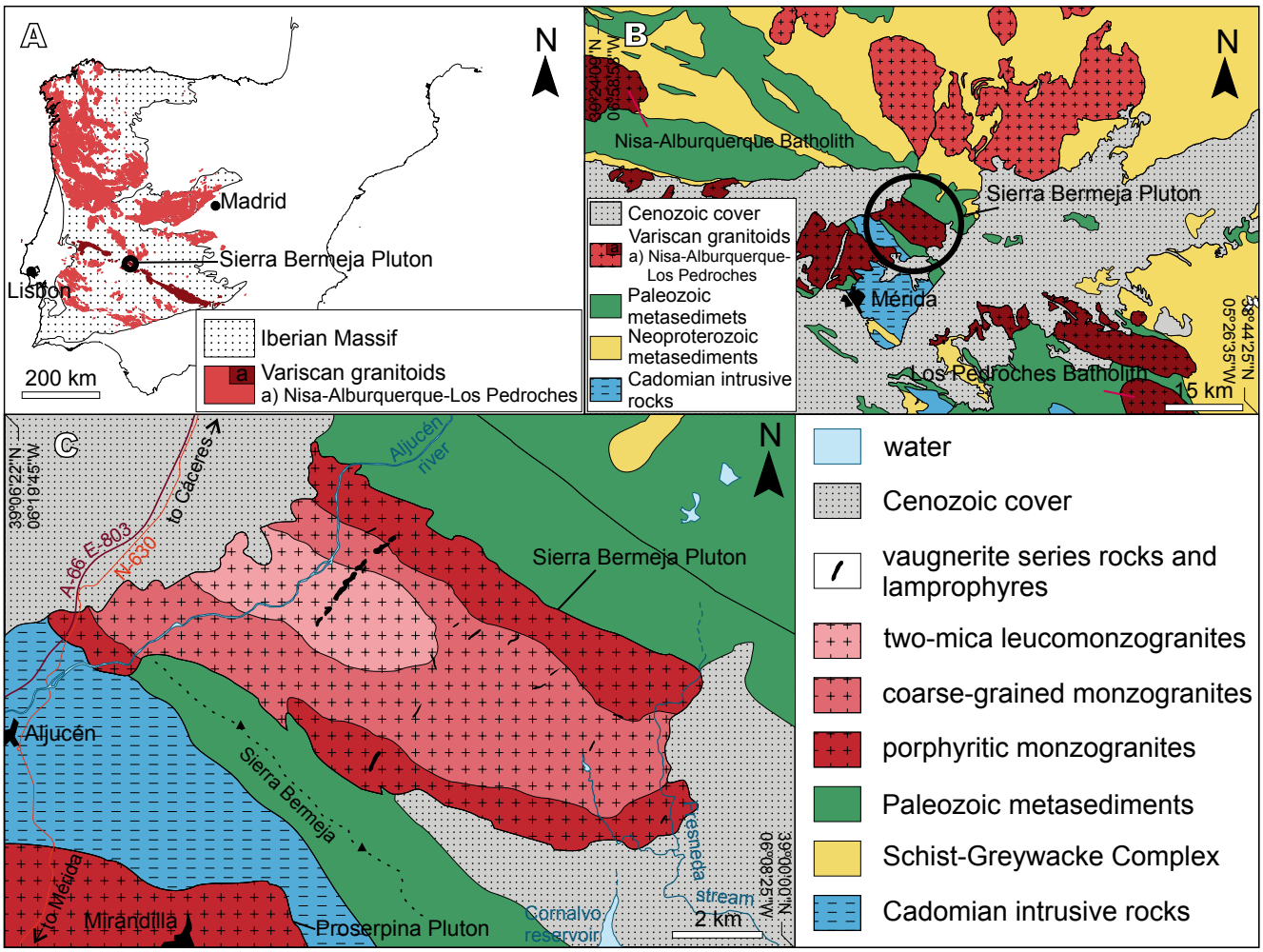

FIGURE 1. A) Geological sketch map of the Variscan granitoids in the Iberian Massif; the Nisa-Alburquerque-Los Pedroches Magmatic Alignment is emphasised. B) Regional geologic map of the central area of the Nisa-Alburquerque-Los Pedroches Magmatic Alignment (adapted from Palacios *et al.*, 2013). C) Geological sketch map of the Sierra Bermeja Pluton (host rocks and Cenozoic cover adapted from López Sopena *et al.*, 1990; Del Olmo Sanz *et al.*, 1992).

This pluton is emplaced in the Alcudian Domain of the southernmost Central Iberian Zone, intruding the Alegrete-San Pedro de Mérida-Montoro thrust (*e.g.* Eguiluz *et al.*, 2005; Palacios *et al.*, 2013). The host metasedimentary sequence in this region is represented, from base to top, by: i) a thick Neoproterozoic-Lower Cambrian succession of shales and sandstones, known in the regional literature as Schist and Greywacke Complex (Complexo Xisto-Grauváquico by Carrington da Costa, 1950) that crops out in the core of large scale WSW–ENE trending antiforms (Rodríguez Alonso *et al.*, 2004; Palacios *et al.*, 2013); ii) Ordovician-Devonian quartzite and slaty formations deposited on a marine platform unconformably covering the Schist and Greywacke Complex and iii) syn-orogenic Upper Devonian-Carboniferous Culm Facies turbidites deposited in intracontinental, shallow marine basins that unconformably cover the Lower-Middle Paleozoic sequences (Rodríguez Alonso *et al.*, 2004; Palacios *et al.*, 2013).

At a regional scale, it stands out the Variscan Nisa-Alburquerque-Los Pedroches Magmatic Alignment, where the Sierra Bermeja Pluton is included. This alignment is constituted by a series of late-Variscan granitoids that crop out along ≈400km in N140E direction (Fig. 1A). The intrusions comprise predominantly K-rich calc-alkaline biotite ± amphibole granodiorites (*e.g.* Los Pedroches granodiorite) and peraluminous two-mica ± cordierite monzogranites (Gonzalo, 1987; Carracedo, 1991; González Menéndez, 1998; Larrea, 1998; Alonso Olazabal, 2001). The peraluminous monzogranites constitute circumscribed epizonal zoned plutons, emplaced generally later than the K-rich calc-alkaline granodiorites. These cordierite-bearing monzogranites (known in the regional literature as 'Serie Mixta' granitoids) have mostly features of S-type granites, although they also show some I-type granite characteristics, which difficult their genetic interpretation (*e.g.* Corretgé *et al.*, 1977; Castro *et al.*, 2002; Bea, 2004).

FIELD CHARACTERISTICS

The Sierra Bermeja Pluton is constituted by massive and apparently isotropic monzogranites characterised by the presence of relatively abundant euhedral cordierite crystals. The new mapping of this pluton has shown that it is composed of three main monzogranitic units that present a roughly concentric arrangement in map view and correspond, from the outermost areas towards the central part of the pluton, to: i) porphyritic monzogranites; ii) coarse-grained monzogranites and iii) two-mica leucomonzogranites (Fig. 1C). Field observations indicate their close time of emplacement, depicting intrusive relationships that generated narrow mingling zones along their contacts.

The three granitic facies bear mafic rocks not previously described that appear as longitudinal alignments of variable length (10–1000m) and width (1–30m) inside them. Although at the used map scale these mafic rocks are arranged following rectilinear paths oriented N020–040E, at the outcrop scale their trace is irregular, sinuous and discontinuous, at times even with strong curvatures. In detail, each elongated mass is defined in turn by alignments of small (diameter of 0.5–1m), rounded, dark-coloured blocks, which stand out against the light-coloured granitic sandy ground. The spacing of the mafic blocks at the outcrop varies between 0.5m and 3m (Fig. 2A, B); indeed, they do not constitute continuous masses and the spacing between blocks increases progressively towards the ends of the alignments up to finally disappear. It may be noted that, at the outcrop scale, these dark-coloured rocks do not show any positive relief, and usually appear even in plains or slight depressions and always confined within the boundaries of the pluton (Fig. 1C).

The elongated dark-coloured bodies are constituted by massive and apparently isotropic rocks, which, according to their field textural, mineralogical and modal features, are categorised in two end-member types, one aphanitic and another phaneritic. The first type, which represents most of the bodies (26 out of the 33 studied bodies) and usually forms rectilinear narrow (<5m) alignments, is formed by aphanitic rocks with porphyritic texture, characterised by the presence of clinopyroxene phenocrysts (up to 6mm-long) included in a microcrystalline groundmass. Commonly, these aphanitic rocks exhibit quartz xenocrystals and, occasionally, enclaves of monzogranite (Fig. 2C). The second type of mafic rocks, which forms the widest (>10m) bodies and is mainly restricted to the principal alignment in the western part of the pluton, is constituted by phaneritic rocks with a medium-grained gabbroic texture. It may be noted that each observed alignment is always composed by just one of the aforementioned end members, that is, either aphanitic or phaneritic, showing homogeneous appearance in terms of textural variations along and across the body. Indeed, in those alignments constituted by the phaneritic facies, the crystal sizes remain constant up to the border of the bodies.

METHODS

Fourteen representative samples of the outcrops of mafic rocks found in the Sierra Bermeja Pluton have been selected for the present study. The petrographic observations in thin section (50 thin sections: 29 of them corresponding to the aphanitic terms, and 21 to the phaneritic ones) have been made with a polarising microscope Leica DM LP model fitted with a CCD camera. Mineral phase proportions have been obtained by means of modal counting (2000 points/sample in phaneritic rocks and 600 points/sample in the aphanitic ones; Table 1). Major element determinations in mineral phases have been performed on polished thin sections by electron microprobe techniques at the University of Oviedo using a Cameca SX100 instrument (Tables 2; 3; 4; 5). Operating conditions of the microprobe have been: 10s counting time (peak), ≈10nA beam current and 15kV accelerating voltage. Calibration has been done against French Geological Survey (BRGM) standard minerals and matrix correction factors (PAP) have been used. Among the 14 samples of mafic rocks, we have selected 10 (6 aphanitic and 4 phaneritic) for whole-rock major and trace element analyses (Table 6) which have been performed by Inductively Coupled Plasma-Optical Emission Spectrometry (ICP-OES; Perkin Elmer Optima 8300) and Inductively Coupled Plasma-Mass Spectrometry (ICP-MS; Thermo Fisher XSeries 2) at the Geochronology and Isotope Geochemistry SGIker-Facility of the UPV/EHU, following procedures adapted from those described in detail in García de Madinabeitia *et al.* (2008).

PETROGRAPHY

The mafic rocks that form alignments within the Sierra Bermeja Pluton are composed by variable amounts of the following minerals: plagioclase, amphibole, clinopyroxene, biotite, K-feldspar, quartz, apatite, titanite, zircon, allanite, pyrite, ilmenite and chromite. Secondary mineralogy consists of epidote, titanite, calcite, chlorite, sericite and carbonate minerals. Qualitatively, the mineralogy is fairly homogeneous but, as pointed out earlier, each alignment is composed by either aphanitic or phaneritic rocks whose main differences in petrography are described below.

The aphanitic rocks are mesocratic (colour index 44–54) and show holocrystalline porphyritic texture (Fig. 3A, B), although phenocrysts are relatively scarce (2–7vol.%) and rarely exceed 2mm in size. Phenocrysts

are represented mostly by clinopyroxene, frequently clustered in aggregates of up to 3mm-long that define a glomeroporphyritic texture and, less often, by amphibole and biotite. Plagioclase phenocrystals (up to 2mm) have been identified only in one sample, sporadically arranged in glomeroporphyritic aggregates. The groundmass is microcrystalline and constituted by these same minerals plus the aforementioned accessory mineralogy. According to their texture and modal contents (see Table 1), the aphanitic, porphyritic rocks may be regarded as lamprophyres, more specifically as kersantites, except for one sample that would be classified as minette. Finally, the sample rich in plagioclase phenocrystals is classified as micro-diorite.

The phaneritic rocks exhibit a mesocratic (colour index: 39–47), fine- to medium-grained (0.5–3mm), hipidio-idiomorphic, inequigranular seriated texture (Fig. 3C–F). Average mineral modal contents (Table 1) reveal the existence of two types of phaneritic rocks: biotite-poor (Fig. 3C, D) and biotite-rich (Fig. 3E; F). In the former, plagioclase (46vol.%) and amphibole (29vol.%) are the main constituents, followed by clinopyroxene (14vol.%) and K-feldspar (6vol.%), whereas accessory phases are titanite, zircon, allanite, pyrite, ilmenite, chromite and biotite, standing out their relatively high quartz (5vol.%) and apatite (1vol.%) contents. The apparent absence of biotite in this biotite-poor facies (Table 1) must be taken with caution since some chlorite aggregates enclose traces of biotite microcrystals (<0.3mm) that suggest originally biotite contents were slightly greater than those currently observed (yet <5vol.%). In the biotite-rich terms, plagioclase (46vol.%), biotite (22vol.%), clinopyroxene (22vol.%) and K-feldspar (5vol.%) are the main constituents, followed by minor contents of quartz (2vol.%), amphibole (2vol.%) and apatite (1vol.%), besides the accessories allanite, pyrite, titanite, zircon, ilmenite and chromite. Following Le Maitre *et al.* (2002) these phaneritic rocks are classified as diorites, quartz diorites and quartz monzodiorites (from this point forward we will use the term 'dioritoids' in order to simplify).

Particular textures

In addition to the main ones described above, a number of particular textures have been recognized under the optical microscope as listed hereafter: i) Quartz ocelli (Fig. 4A) formed by relatively large quartz crystals (up to 3mm), which occasionally exhibit crystal embayments, surrounded by a rim of amphibole and clinopyroxene crystals. The quartz ocelli are more common in the lamprophyres, while the rest of particular microstructures are more frequent in the dioritoids; ii) globular textures, constituted by plagioclase, quartz and alkali feldspar aggregates (up to 2mm in diameter) encircled by a rim of amphibole crystals; iii) feldspar crystals showing patchy alteration to epidote (Fig. 4B); iv) coexisting stubby prismatic and acicular apatite; v) clinopyroxene clots, constituted by a central, subidiomorphic clinopyroxene crystal (up to 2mm) surrounded by a polycrystalline rim of amphibole and opaque minerals (Fig. 4C); vi) sparse felsic segregations, constituted by K-feldspar, plagioclase,

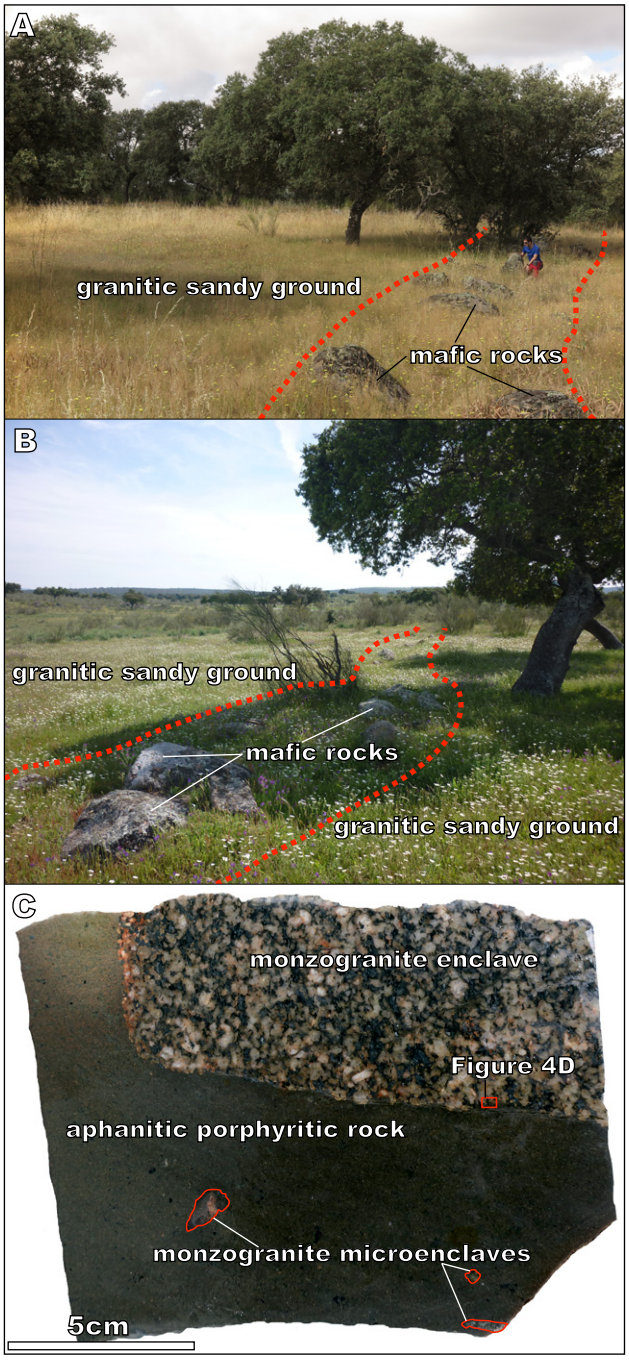

FIGURE 2. A) and B) Field characteristics of the mafic rock alignments that crop out in the Sierra Bermeja Pluton. C) Scanned image of a polished hand sample of lamprophyre enclosing a decimetric monzogranite enclave and microenclaves.

TABLE 1. Representative modal compositions (in vol. %) of the mesocratic rocks of the Sierra Bermeja Pluton

Rock-type	Lamprophyre				Dioritoid (Vaugnerite*)					Micro-dt
	Mnt	Krs	Krs	Krs	Bt-r	Bt-r	Bt-p	Bt-p	Bt-p	
Sample	1522	1570	1638	1643	1606	1703	1604	1641	1701	1540
Pl	9.6	50.5	42.8	54.4	50.5	43.5	43.6	48.7	38.7	55.3
Cpx	6.7	8.8	15.6	12.3	24.0	19.6	13.9	9.2	14.9	4.9
Bt	18.7	26.2	21.7	19.2	21.9	21.7	0.3	-	-	0.5
Amp	1.1	13.7	16.1	12.2	-	2.5	25.1	32.5	27.7	31.9
Kfs	54.9	-	2.4	0.3	2.0	7.6	9.2	3.3	12.9	0.6
Qz	5.6	-	0.9	0.8	0.3	2.7	6.4	3.3	5.7	2.8
Ap	1.6	-	0.3	0.3	0.6	1.3	1.4	1.5	0.3	1.3
Opq	1.8	0.8	0.2	0.3	0.4	1.1	0.1	1.2	-	2.7
Other	-	-	-	-	0.4	-	-	0.5	-	-

*See Discussion section for the consideration of dioritoids as vaugnerites. Mnt (minette); Krs (kersantite); Bt-r (biotite-rich); Bt-p (biotite-poor); Micro-dt (micro-diorite); Pl (plagioclase); Cpx (clinopyroxene); Bt (biotite); Amp (amphibole); Kfs (K-feldspar); Qz (quartz); Ap (apatite); Opq (opaque mineral).

quartz and lesser amounts of amphibole, characterised by their lack of pyroxene crystals. The outer limits of these segregates are very irregular and diffuse (Fig. 4C); vii) finally, it may be noted the occasional existence of microenclaves of host monzogranite characterised by their irregular and diffuse external limits (Figs. 2C; 4D).

MINERAL CHEMISTRY

In the mineralogical characterisation that follows we have considered both types of mafic rocks within the Sierra Bermeja Pluton, lamprophyres and dioritoids.

Microprobe analytical data of clinopyroxenes reveal they are of Ca-Mg-Fe type (Morimoto, 1988), with relatively narrow compositional variations: $Wo_{38–47}En_{37–51}Fs_{10–17}$. In the biotite-rich dioritoids the pyroxenes correspond mostly to diopside, whereas in the biotite-poor terms they are mostly augite (Fig. 5A). Pyroxenes in the lamprophyres classify as augite (Fig. 5A). TiO_2 contents and $Mg^{\#}$ values in lamprophyres vary between 0.42–1.91wt.% and 0.74–0.83, respectively, while in the dioritoids these value ranges are slightly wider: TiO_2=0.05–2.80wt.%; $Mg^{\#}$=0.48–0.79. In detail, $Mg^{\#}$ values are slightly higher in the biotite-poor dioritoids respect to those of the biotite-rich dioritoid. Cr contents

TABLE 2. Representative pyroxene compositions from the mesocratic rocks of the Sierra Bermeja Pluton

Rock-type	Lamprophyre			Dioritoid (Vaugnerite*)				Micro-dt
	Mnt	Krs	Krs	Bt-r	Bt-r	Bt-p	Bt-p	
Sample	1522	1570	1570	1606	1606	1641	1642	1540
SiO_2	51.15	50.98	50.88	47.98	49.49	50.66	49.35	48.37
TiO_2	1.03	0.57	0.58	1.99	1.44	1.15	1.36	1.91
Al_2O_3	2.60	4.11	4.27	4.98	3.77	2.90	3.67	5.11
Cr_2O_3	0.80	0.74	0.73	0.06	0.08	0.10	0.18	0.07
NiO	0.03	0.03	0.03	0.00	0.00	0.04	0.00	0.03
FeO	6.97	6.57	5.95	9.41	8.51	7.81	7.90	8.61
MnO	0.19	0.17	0.14	0.30	0.24	0.20	0.18	0.20
MgO	15.66	16.86	16.25	12.61	13.95	15.07	14.36	13.47
CaO	20.98	18.61	20.22	21.20	21.33	21.11	21.66	21.10
Na_2O	0.22	0.56	0.49	0.44	0.38	0.33	0.41	0.48
K_2O	0.00	0.00	0.01	0.00	0.00	0.00	0.02	0.01
Total	99.63	99.19	99.54	98.98	99.19	99.37	99.10	99.38
Wo	43.39	39.32	42.50	45.76	44.84	43.68	45.17	45.16
En	45.05	49.57	47.51	37.87	40.80	43.39	41.66	40.11
Fs	11.56	11.11	9.99	16.37	14.36	12.93	13.16	14.72

*See Discussion section for the consideration of dioritoids as vaugnerites. Mnt (minette); Krs (kersantite); Bt-r (biotite-rich); Bt-p (biotite-poor); Micro-dt (micro-diorite).

TABLE 3. Representative amphibole compositions from the mesocratic rocks of the Sierra Bermeja Pluton

Rock-type	Lamprophyre		Dioritoid (Vaugnerite*)					Micro-dt	
	Krs	Krs	Bt-r	Bt-p	Bt-p	Bt-p	Bt-p		
Sample	1570	1570	1606	1642	1641	1642	1642	1540	1540
SiO_2	40.05	39.83	40.45	40.55	40.15	41.32	40.60	39.23	39.07
TiO_2	3.71	4.37	5.07	4.53	5.07	3.83	4.28	5.29	4.95
Al_2O_3	12.24	13.54	11.52	11.46	11.78	10.76	11.46	12.26	11.84
Cr_2O_3	0.00	0.01	0.00	0.01	0.06	0.01	0.01	0.01	0.00
NiO	0.00	0.01	0.02	0.00	0.00	0.08	0.00	0.03	0.00
FeO	13.21	10.23	13.83	13.01	12.33	15.23	13.26	11.77	14.96
MnO	0.13	0.14	0.19	0.18	0.16	0.25	0.23	0.16	0.20
MgO	12.39	13.52	10.94	12.25	12.57	11.26	12.09	12.61	10.37
CaO	11.41	11.52	11.77	11.54	11.72	10.87	11.43	11.41	11.25
Na_2O	2.06	1.97	2.58	2.38	2.27	2.36	2.30	2.33	2.30
K_2O	1.34	1.64	1.11	1.27	1.25	1.10	1.26	1.06	1.28
F	0.15	0.21	N.A.	N.A.	N.A.	N.A.	N.A.	0.17	0.13
Cl	0.06	0.05	N.A.	N.A.	N.A.	N.A.	N.A.	0.02	0.02
Total	96.75	97.06	97.49	97.17	97.35	97.08	96.91	96.36	96.37

*See Discussion section for the consideration of dioritoids as vaugnerites. Krs (kersantite); Bt-r (biotite-rich); Bt-p (biotite-poor); Micro-dt (micro-diorite); N.A. (not analysed).

are slightly higher in the augites of the lamprophyres (up to 0.90wt.% Cr_2O_3) than in the diopsides of dioritoids (up to 0.46wt.%).

Amphiboles of lamprophyres and dioritoids classify as kaersutite and pargasite (Fig. 5B), although some edenite and Mg-hornblende are present occasionally in the dioritoids. TiO_2 and Cr_2O_3 average contents in amphiboles of dioritoids (4.79wt.% and 0.04wt.%, respectively) are slightly higher than in the lamprophyres (4.37wt.% and <0.01wt.%), as are average contents of Na_2O (2.31wt.% and 2.15wt.%, respectively). Finally, $Mg^{\#}$ values are practically similar in both types of rocks, ranging 0.55–0.71.

TABLE 4. Representative biotite compositions from the mesocratic rocks of the Sierra Bermeja Pluton

Rock-type	Lamprophyre			Dioritoid (Vaugnerite*)			Micro-dt	
	Krs	Krs	Krs	Bt-r	Bt-r	Bt-r		
Sample	1570	1570	1570	1606	1606	1606	1540	1540
SiO_2	34.70	35.86	36.39	35.87	35.80	35.45	35.00	34.40
TiO_2	5.85	5.56	4.57	5.16	5.78	5.99	6.31	6.79
Al_2O_3	14.85	15.04	14.97	14.50	14.61	14.15	14.92	14.50
Cr_2O_3	0.03	0.09	0.00	0.04	0.00	0.02	0.03	0.02
NiO	0.01	0.00	0.03	0.00	0.00	0.03	0.00	0.00
FeO	19.65	11.68	13.99	14.76	15.57	17.61	14.35	18.26
MnO	0.16	0.06	0.12	0.06	0.10	0.13	0.08	0.11
MgO	9.96	15.35	14.93	14.35	13.50	11.51	12.72	10.20
CaO	0.18	0.06	0.04	0.02	0.01	0.01	0.06	0.10
Na_2O	0.13	0.30	0.24	0.47	0.43	0.38	0.15	0.16
K_2O	8.35	8.60	8.55	8.68	8.62	8.59	8.23	8.11
F	0.20	0.31	0.37	0.05	0.17	0.28	0.12	0.07
Cl	0.08	0.04	0.03	0.03	0.04	0.06	0.02	0.02
Total	94.15	92.94	94.23	94.01	94.62	94.20	91.98	92.76
Al(total)**	1.36	1.34	1.33	1.29	1.30	1.28	1.36	1.33
$Mg/(Mg+Fe^{2+})$**	0.49	0.71	0.68	0.66	0.63	0.56	0.62	0.51

*See Discussion section for the consideration of dioritoids as vaugnerites. Krs (kersantite); Bt-r (biotite-rich); Micro-dt (micro-diorite).

** a.p.f.u. (atoms per formula unit)

TABLE 5. Representative feldspar compositions from the mesocratic rocks of the Sierra Bermeja Pluton

Rock-type	Lamprophyre			Dioritoid (Vaugnerite*)					Micro-dt
	Mnt	Krs	Krs	Bt-r	Bt-p	Bt-p	Bt-p	Bt-p	
Sample	1522	1570	1570	1606	1642	1642	1641	1641	1540
SiO_2	65.05	57.92	52.82	66.33	66.79	65.40	67.25	64.40	53.09
TiO_2	0.01	0.00	0.05	0.01	0.02	0.01	0.00	0.02	0.06
Al_2O_3	18.40	26.04	28.78	21.26	20.70	17.90	20.45	18.39	29.37
Cr_2O_3	0.00	0.00	0.03	0.00	0.01	0.00	0.05	0.00	0.00
NiO	0.00	0.00	0.00	0.00	0.00	0.00	0.00	0.00	0.00
FeO	0.15	0.31	0.55	0.12	0.06	0.03	0.00	0.05	0.47
MnO	0.00	0.01	0.00	0.02	0.00	0.02	0.01	0.02	0.00
MgO	0.00	0.02	0.12	0.00	0.00	0.00	0.01	0.00	0.08
CaO	0.03	8.97	12.89	2.09	2.04	0.01	0.88	0.00	12.58
Na_2O	0.27	6.17	3.92	10.27	10.37	0.39	11.77	0.26	4.07
K_2O	16.24	0.56	0.44	0.25	0.16	15.92	0.05	16.77	0.42
Total	100.15	100.00	99.59	100.35	100.15	99.67	100.48	99.91	100.16
Or	97.37	3.19	2.58	1.43	0.91	96.38	0.29	97.66	2.47
Ab	2.48	53.66	34.57	88.61	89.39	3.59	95.75	2.34	36.03
An	0.15	43.15	62.85	9.95	9.70	0.03	3.96	0.00	61.50

*See Discussion section for the consideration of dioritoids as vaugnerites. Mnt (minette); Krs (kersantite); Bt-r (biotite-rich); Bt-p (biotite-poor); Micro-dt (micro-diorite).

The biotites of dioritoids are classified as biotite *s.s.* with $Mg^{\#}$=0.56–0.66, whereas in the lamprophyres, with $Mg^{\#}$=0.49–0.77, several analyses plot in the phlogopite field (Fig. 5C). Although the biotites of both rock types are very similar, the compositional ranges are larger in the lamprophyres than in the dioritoids (*e.g.* FeO_t=9.31–19.64wt.% *vs.* 14.76–17.60wt.%).

Alkali feldspar is always very homogeneous ($Or_{94–98}$) and plots for both rock types are close to the orthoclase vertex in the An–Ab–Or diagram (Fig. 5D). The cores of plagioclases in the dioritoids are highly altered which precludes a proper characterisation, while the rims exhibit marked albitic to oligoclase compositions ($An_{03–26}$). On the contrary, plagioclases of lamprophyres are better preserved and classify as andesine-labradorite (An_{43}–An_{63}; Fig. 5D).

Finally, analysed opaque minerals in both groups of rocks correspond to ilmenite, pyrite and chromite.

WHOLE-ROCK GEOCHEMISTRY

Ten samples, 5 lamprophyres, 1 micro-diorite, 1 biotite-rich and 3 biotite-poor dioritoids were selected for the whole-rock geochemical characterisation of the mesocratic rocks from the Sierra Bermeja Pluton (Table 6).

Major element geochemistry

Lamprophyres are rocks of intermediate composition (SiO_2=55.13–56.11wt.%), metaluminous (A/CNK=0.71–0.91), potassium- and calcium-rich (K_2O=3.98–4.74wt.%; CaO=4.51–5.84wt.%) and with lower contents of sodium (Na_2O=2.16–2.78wt.%) than potassium. They plot close to the line of Irvine and Baragar (1971) that separates alkaline and subalkaline rocks in the Total Alkali Silica (TAS) diagram (Le Maitre *et al.*, 2002), integrating in a possible transitional association (Fig. 6A). They exhibit relative high titanium (TiO_2=1.12–1.56wt.%) and low *mg* values [100*MgO/(MgO+FeO)=41–48], which is consistent with their more ferroan (total iron as Fe_2O_3=6.16–7.53wt.%) than magnesian (MgO=3.99–6.18wt.%) character. From a geochemical point of view, the lamprophyres are as a whole classified as latites (Le Maitre *et al.*, 2002).

The biotite-rich dioritoid is a basic rock (SiO_2=48.93wt.%), whereas the biotite-poor dioritoids and the micro-diorite are intermediate (SiO_2=50.92–53.83wt.%). All these rocks are metaluminous (A/CNK=0.71 for the biotite-rich and 0.76–0.80 for the biotite-poor) and calcium-rich (CaO=7.09wt.% for the biotite-rich and 5.61–5.90wt.% for the biotite-poor), with relatively similar contents of potassium (2.65wt.% K_2O and 2.92–3.38wt.%) and sodium (3.04wt.% Na_2O and 3.10–3.30wt.%; the micro-diorite being slightly poorer with 2.56%wt.%). Like the lamprophyres, the dioritoids and micro-diorite of Sierra Bermeja Pluton would be transitional (Fig. 6B) and richer in iron (total as Fe_2O_3=8.22–10.11wt.%) than in magnesium (MgO=5.59–7.59wt.%). It may be noted that the biotite-rich dioritoid presents higher values of titanium (TiO_2=1.85wt.%) and *mg* [100*MgO/(MgO+FeO)=55] than the biotite-poor types (TiO_2=1.51–1.57wt.%;

TABLE 6. Whole-rock compositions of the mesocratic rocks of the Sierra Bermeja Pluton. Major elements are expressed in wt. %, and trace elements in ppm

Rock-type	Lamprophyre					Dioritoid (Vaugnerite*)				Micro-dt
	Mnt	Krs	Krs	Krs	Krs	Bt-r	Bt-p	Bt-p	Bt-p	
Sample	1522	1570	1612	1638	1643	1606	1603	1641	1642	1540
SiO_2	55.53	55.35	55.59	55.13	56.11	48.93	53.29	53.83	53.35	50.92
TiO_2	1.56	1.13	1.51	1.12	1.14	1.85	1.51	1.51	1.57	1.67
Al_2O_3	15.52	15.81	14.21	13.72	14.42	14.66	14.61	14.57	15.21	14.93
$Fe_2O_3^t$	6.88	6.16	7.37	7.53	7.00	10.11	8.60	8.22	9.02	8.53
MnO	0.13	0.09	0.11	0.12	0.10	0.14	0.12	0.12	0.13	0.12
MgO	4.27	3.99	5.58	6.18	4.75	7.59	6.12	5.59	5.97	5.73
CaO	4.51	4.92	5.19	5.84	5.35	7.09	5.83	5.61	5.90	6.41
Na_2O	2.26	2.55	2.16	2.64	2.78	3.04	3.10	3.30	3.25	2.56
K_2O	4.68	4.74	4.33	4.07	3.98	2.65	3.09	3.38	2.92	3.24
P_2O_5	0.70	0.72	0.75	0.74	0.53	0.69	0.70	0.63	0.65	0.65
LOI	3.18	3.76	2.56	2.27	3.66	2.65	2.37	2.20	2.54	4.64
TOTAL	99.22	99.22	99.36	99.36	99.82	99.40	99.34	98.96	100.51	99.40
Ba	1504	2095	1271	1466	1644	963	1552	1041	1039	1177
Co	35.8	34.0	32.3	37.1	29.4	41.5	42.5	44.8	36.4	44.3
Cr	324	87.0	330	224	171	230	222	179	184	221
Cs	11.5	13.4	16.3	11.2	11.2	9.12	1.65	2.87	3.30	153
Ga	25.7	23.8	21.1	19.8	18.4	19.2	21.2	18.9	18.3	23.7
Hf	8.35	9.13	8.15	9.06	10.8	6.13	7.10	7.24	6.86	5.33
Nb	17.8	19.9	17.2	20.0	19.7	22.3	24.9	23.4	22.7	18.9
Ni	14.3	8.68	12.0	55.7	66.6	87.9	67.5	58.0	57.7	72.5
Pb	28.9	31.0	22.9	30.3	31.4	19.5	16.8	17.1	18.9	23.9
Rb	368	226	306	207	162	105	88.7	99.2	87.7	260
Sc	20.5	17.7	22.2	20.4	17.4	20.9	18.0	19.4	20.0	18.6
Sn	5.65	3.06	10.5	6.70	3.66	2.39	3.43	4.14	3.31	5.69
Sr	401	1149	455	810	680	778	750	739	800	774
Ta	1.34	1.59	1.14	1.59	1.38	1.50	1.86	1.80	1.70	1.46
Th	31.0	31.4	25.2	37.6	33.7	10.0	14.5	13.0	12.0	15.3
U	8.85	9.72	6.49	9.75	7.81	2.73	4.86	4.54	4.19	5.76
V	142	142	155	162	127	157	134	128	132	128
Y	39.7	32.6	30.6	28.5	28.4	30.4	34.3	31.1	31.2	40.4
Zn	93.3	68.8	89.0	68.3	61.5	87.5	86.0	71.8	75.2	94.7
Zr	341	355	372	341	394	276	310	294	272	239
La	51.3	76.6	41.7	59.4	65.7	48.8	63.0	63.9	58.6	66.4
Ce	119	164	96.0	136	133	98.8	140	126	117	142
Pr	16.5	20.0	13.2	15.7	16.6	12.6	15.6	15.7	15.0	17.4
Nd	71.7	80.3	56.9	63.0	64.5	49.8	61.1	61.3	59.3	70.9
Sm	13.9	13.1	10.7	10.4	10.7	8.93	10.4	10.8	10.6	12.4
Eu	2.93	3.08	2.32	2.33	2.27	2.22	2.56	2.46	2.41	2.94
Gd	9.96	9.65	7.85	7.54	7.44	7.42	8.52	7.96	7.87	10.0
Tb	1.31	1.17	0.973	0.927	0.960	0.963	1.07	1.06	1.04	1.34
Dy	6.57	5.68	5.26	4.91	4.88	5.25	5.83	5.43	5.42	6.84
Ho	1.00	0.852	0.882	0.821	0.750	0.885	0.974	0.820	0.820	1.01
Er	3.12	2.65	2.57	2.35	2.28	2.51	2.78	2.47	2.48	3.13
Tm	0.492	0.396	0.381	0.350	0.360	0.366	0.407	0.390	0.380	0.469
Yb	2.96	2.44	2.36	2.13	2.16	2.23	2.49	2.31	2.29	2.87
Lu	0.484	0.376	0.365	0.327	0.340	0.340	0.378	0.360	0.350	0.451

*See Discussion section for the consideration of dioritoids as vaugnerites. Mnt (minette); Krs (kersantite); Bt-r (biotite-rich); Bt-p (biotite-poor); Micro-dt (micro-diorite).

[(100*MgO/(MgO+FeO)]=42–44). According to the TAS diagram (Middlemost, 1994) the biotite-poor samples would be classified as monzodiorites and monzonites, whereas the biotite-rich dioritoid and the micro-diorite would correspond to monzodiorites (Fig. 6B).

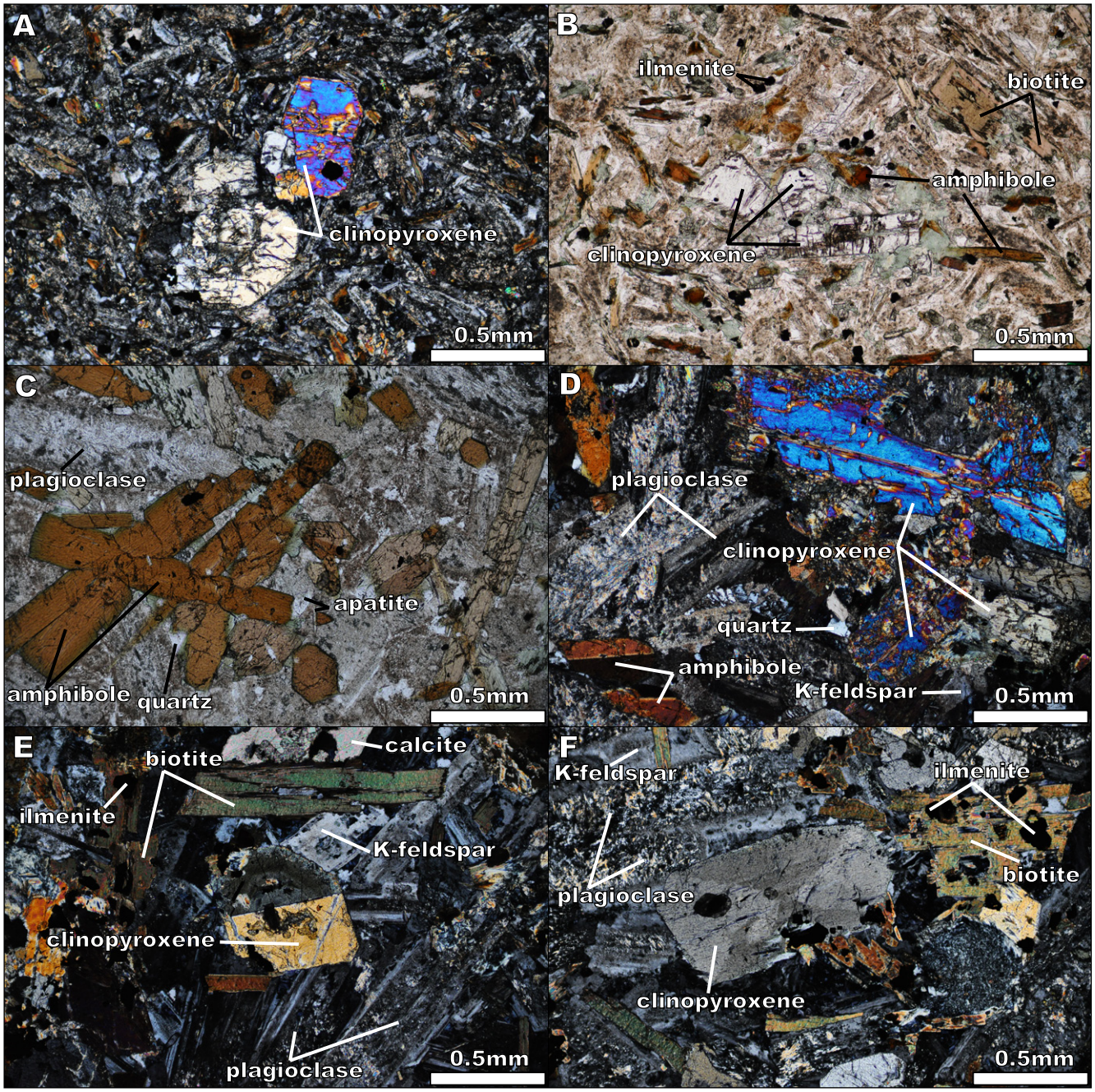

FIGURE 3. Optical microphotographs (A, D, E and F in cross-polarised light, B and C in plane-polarised light). A) and B) Lamprophyre showing glomeroporphyritic texture of clinopyroxene (A), and clinopyroxene and biotite phenocrystals (B). C) Elongated brown amphibole aggregates in a biotite-poor dioritoid. D) Representative texture of a biotite-poor dioritoid. E) and F) Representative images of a biotite-rich dioritoid.

Trace element geochemistry

Trace elements composition of lamprophyres is very variable showing in cases high values of Cr (87–330ppm), Ni (8.7–66.6ppm), Rb (162–368ppm) and Sr (401–1149ppm). It is also noticeable their relatively high concentrations in Ba (1271–2095ppm), Th (25.17–37.60ppm) and Zr (341–394ppm). Primitive mantle-normalised multielemental diagrams (normalisation values are from Sun and McDonough, 1989) show steep trends characterised by marked enrichments in LILE (>100x primitive mantle) respect to High Field Strength Elements (HFSE, Fig. 6C). These normalised plots show a strong positive anomaly in Pb and, in a lesser extent, Nd (Fig. 6C); in addition, they are also characterised by their marked negative anomalies in Nb and, though less pronounced, Ti and Sr (Fig. 6C).

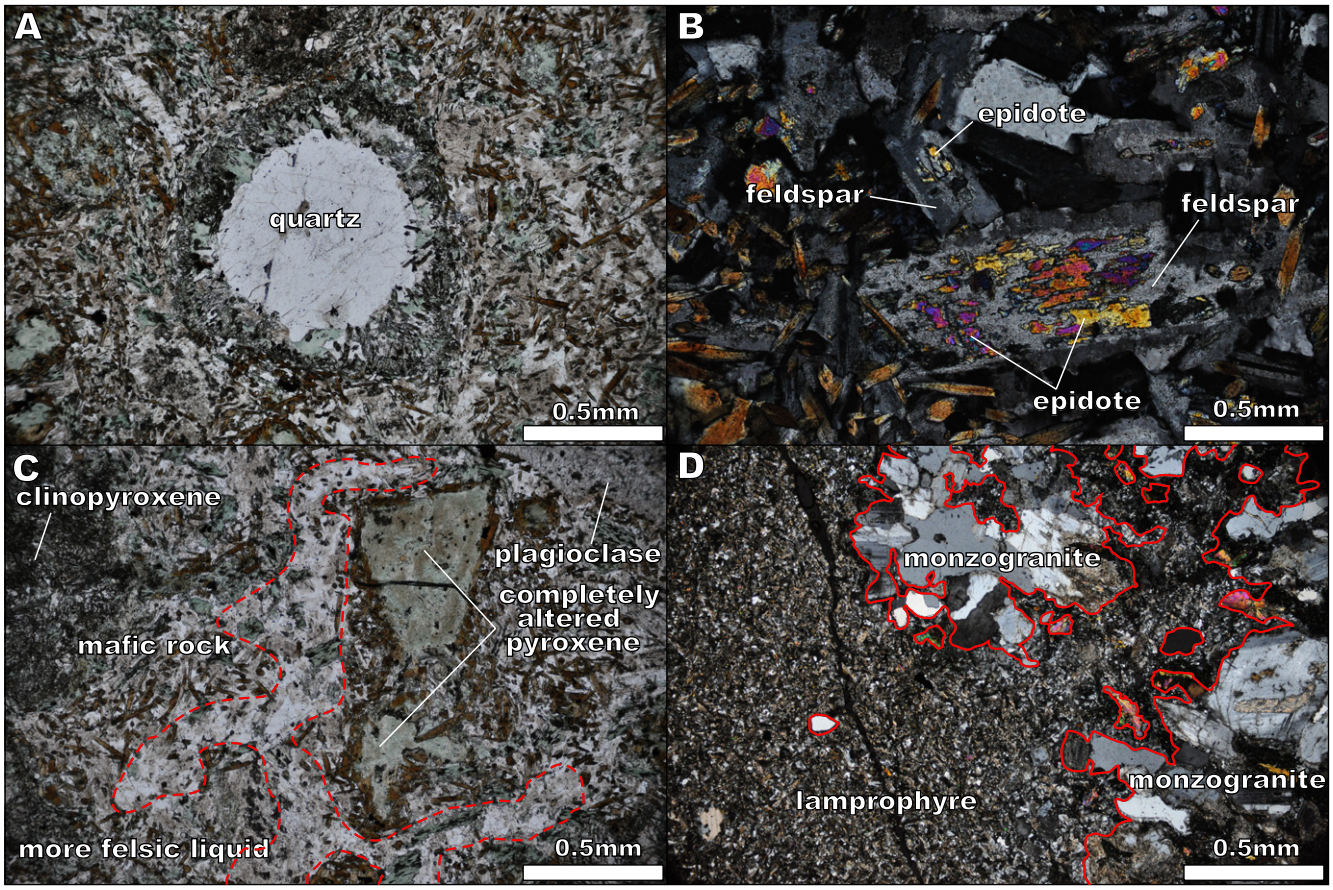

FIGURE 4. Particular microtextures in the mesocratic rocks of the Sierra Bermeja Pluton. A) Quartz ocelli in a lamprophyre. B) Patchy alteration to epidote in plagioclase of dioritoid. C) Clinopyroxene clots and felsic veins (delimited by the dashed line) in lamprophyre. D) Contact between a monzogranite enclave and a host lamprophyre.

Total Rare Earth Element (REE) contents in lamprophyres are relatively high (ΣREE=242–380ppm), but particularly in Light REE (LREE=219–354ppm) compared with Heavy REE (HREE=19–26ppm). The chondrite-normalised diagrams (normalisation values are from Sun and McDonough, 1989) show highly fractionated [$(La/Yb)_N$=12.42–22.49] and segmented patterns, with steep slopes for LREE $(La/Sm)_N$=2.38–3.96) and HREE until Ho [$(Gd/Yb)_N$=2.75–3.27], and nearly flat for the rest of the HREE (Fig. 6D). All the patterns for lamprophyres show slight Eu negative anomalies (Eu/Eu*=0.76–0.84).

The ranges of trace element contents in the dioritoids and micro-diorite are relatively narrower than in lamprophyres standing out the relatively high concentrations of Ba (963–1552ppm), Sr (739–800ppm) and Zr (272–310ppm), whilst Th (10.02–14.46ppm), Cr (179–230ppm), Ni (57.7–87.9ppm) and Rb (88–105ppm) contents are in general lower than those of lamprophyres. Overall, primitive mantle-normalised multielemental diagrams (Sun and McDonough, 1989) for the dioritoids show steep trends characterised by marked enrichments in LILE (>100x primitive mantle) respect to HFSE (Fig. 6C). Note, however, that the dioritoids are poorer in LILE than lamprophyres, while HSFE contents are very similar in both groups. Normalised plots show also the same marked negative anomaly in Nb and, less pronounced, Ti (Fig. 6C). They also exhibit a marked positive anomaly in Pb and a slighter one in Nd but, contrary to lamprophyres they lack a Sr negative anomaly (Fig. 6C).

Total REE contents of dioritoids (ΣREE=241–315ppm) are similar to those of lamprophyres, with relatively higher LREE contents (219–290ppm) than HREE (20–22ppm). Chondrite-normalised (normalisation values are from Sun and McDonough, 1989) patterns are also similar to those of lamprophyres (Fig. 6D), showing strongly fractionated [$(La/Yb)_N$=15.69–19.84] and segmented trends with higher fractionation of LREE [$(La/Sm)_N$=3.46–3.90] than HREE [$(Gd/Yb)_N$=2.75–2.88]. As the lamprohyres, normalised patterns of dioritoids show slight Eu negative anomalies (Eu/Eu*=0.81–0.84) and nearly flat profiles after Ho (Fig. 6D). It is remarkable that the minette and the micro-diorite show more enriched patterns in HREE (Fig. 6D).

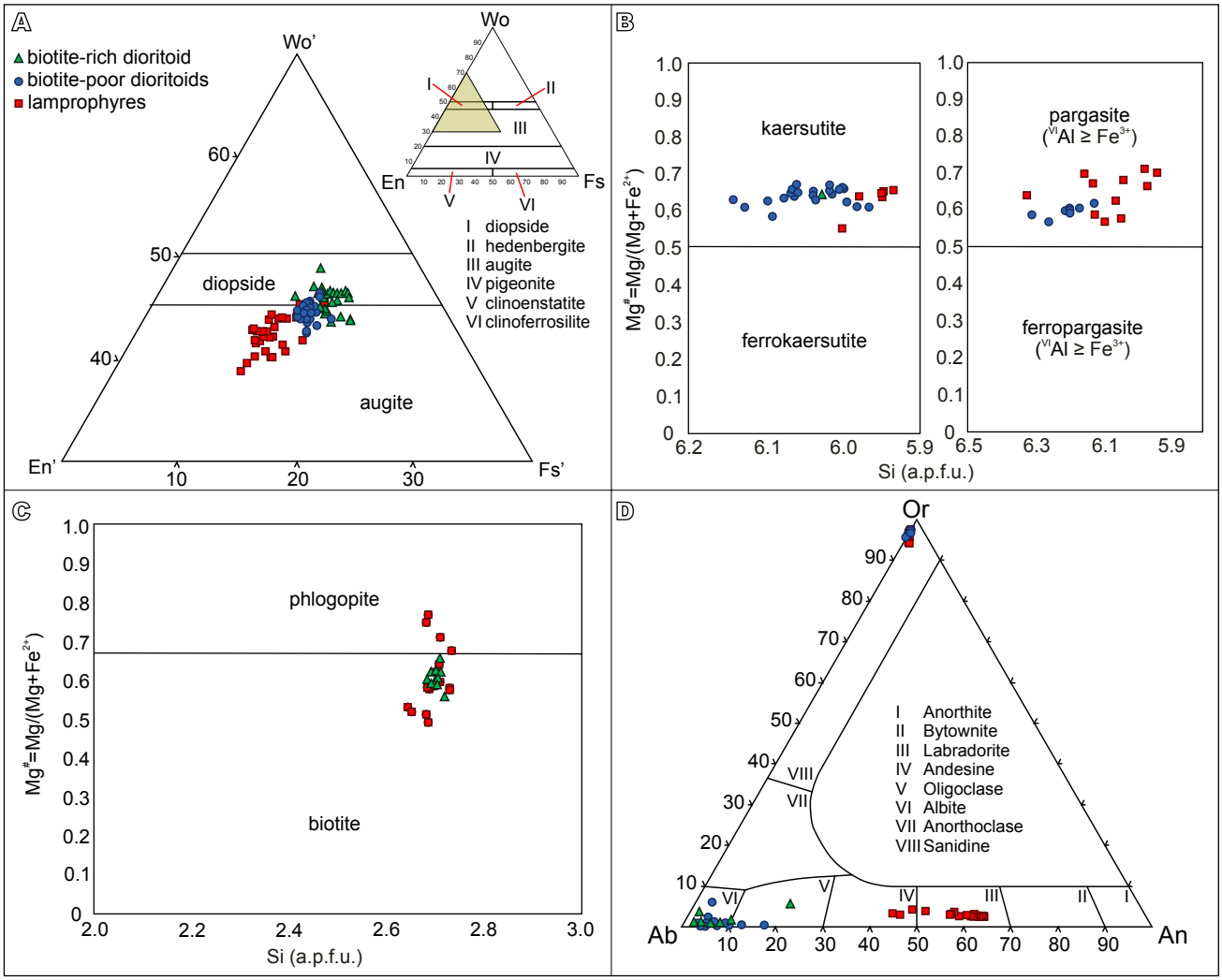

FIGURE 5. Mineral composition diagrams of the mesocratic rocks of the Sierra Bermeja Pluton. A) Wo-En-Fs classification diagram for Ca-Mg-Fe clinopyroxenes (Morimoto, 1988). B) Si *vs.* Mg# classification diagram for calcic amphiboles (Leake *et al.*, 1997). C) Biotite-phlogopite discrimination diagram for biotites *s.l.* (Deer *et al.*, 1962). D) An-Ab-Or classification diagram for feldspars (Deer *et al.*, 1963). The legend for all diagrams is shown in A.

DISCUSSION

On the presence of vaugnerites in the Sierra Bermeja Pluton

Detailed mapping has revealed the existence of two types of intermediate, transitional mesocratic rocks (lamprophyres and dioritoids) emplaced into peraluminous cordierite-bearing monzogranites of the Sierra Bermeja Pluton. Among the mesocratic rocks, the aphanitic terms are classified as kersantites with one as minette and another one as micro-diorite. As for the phaneritic dioritoids, due to their peculiar petrographic and geochemical characteristics, they will be discussed in detail below.

Biotite-rich dioritoids of the Sierra Bermeja Pluton show singular characteristics that fit with those of the vaugnerites described elsewhere in the Variscan Orogen (*e.g.* Sabatier, 1991; Holub, 1997; von Raumer *et al.*, 2014, and references therein). The studied vaugneritic dioritoids exhibit relatively high biotite contents and accessory alkali feldspar and apatite (Table 1). They correspond to basic metaluminous rocks, enriched in LILE (K, Rb, Ba, Sr) and also in FeO_t, MgO and Cr (Table 6). According to these characteristics, they can classify as vaugnerites. On the other hand, the biotite-poor dioritoids from the Sierra Bermeja Pluton, because of their intermediate compositions (Fig. 6A) and their low biotite contents (Table 1), would be in contrast with the 'kind of micaceous diorites' of Sabatier (1991). Nevertheless, the elevated modal amounts of kaersutite and the existence of accessory K-feldspar and apatite (Table 1; Fig. 5B) suggest their vaugneritic nature. This affinity would be also supported by their whole-rock

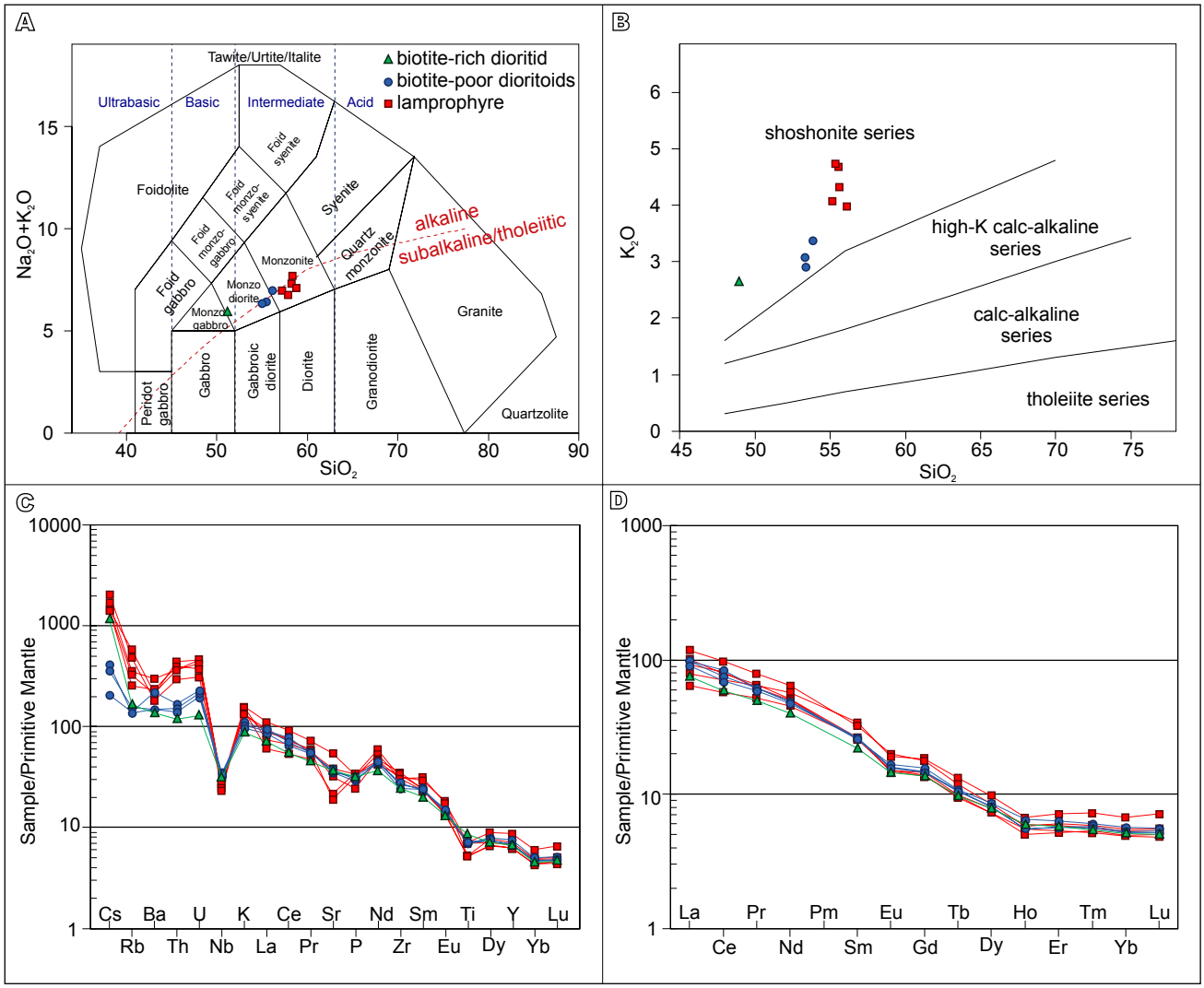

FIGURE 6. A) Projection of lamprophyre and dioritoid compositions in the Total Alkali–Silica (TAS) classification diagram for plutonic rocks (Middlemost, 1994). B) Projection of lamprophyre and dioritoid compositions in the SiO_2 *vs.* K_2O diagram of Peccerillo and Taylor (1976). C) Primitive mantle-normalised diagram of the mesocratic rocks of the Sierra Bermeja Pluton (normalisation values are from Sun and McDonough, 1989). D) Chondrite-normalised REE patterns of the mesocratic rocks of the Sierra Bermeja Pluton (normalisation values are from Sun and McDonough, 1989).

geochemical characteristics, which are very similar to those of the biotite-rich terms (Fig. 6C, D). Consequently, these intermediate rocks may correspond as well to vaugnerites. Finally, despite the fine-grained texture of the micro-diorite, its plagioclase phenocrystals make them different from the lamprophyres of Sierra Bermeja Pluton. In addition, mineral-chemistry data and whole-rock geochemical characteristics are close to those of the dioritoids (Figs. 5; 6), thus, this rock could also be classified as a vaugnerite.

Since 'vaugnerite' is a somewhat generic term as presented in the Introduction section, Rock (1991) and Sabatier (1991) proposed a *mg* [100*MgO/(MgO+FeOt)] *vs. k* [100*K_2O/(K_2O+Na_2O)] comparative diagram for appinites and 'vaugnerite series' rocks (Fig. 7). The dioritoids and micro-diorite of the Sierra Bermeja Pluton plot in the redwitzites and vaugnerite *s.s.* fields, respectively, of the diagram (Fig. 7). In the Iberian Massif (see Introduction for the locations), this kind of Mg- and K-rich rocks are usually categorised as vaugnerites but, as in the case of the Sierra Bermeja Pluton, most of them plot actually in the redwitzite field of the *mg vs. k* diagram (Fig. 7). Only in a few cases, like the granodioritic association of the Tormes Dome (*e.g.* López Plaza *et al.*, 1999; López-Moro *et al.*, 2017), the North of Portugal granites (*e.g.* Dias and Leterrier, 1994; Dias *et al.*, 2002), and in the granites and granodiorites of western Galicia (*e.g.* Gallastegui, 2005) are found some rocks that could be classified as vaugnerites *s.s.* out of the full range of mesocratic rocks in question (Fig. 7). The *mg* values of vaugnerites series rocks of the Sierra Bermeja Pluton are

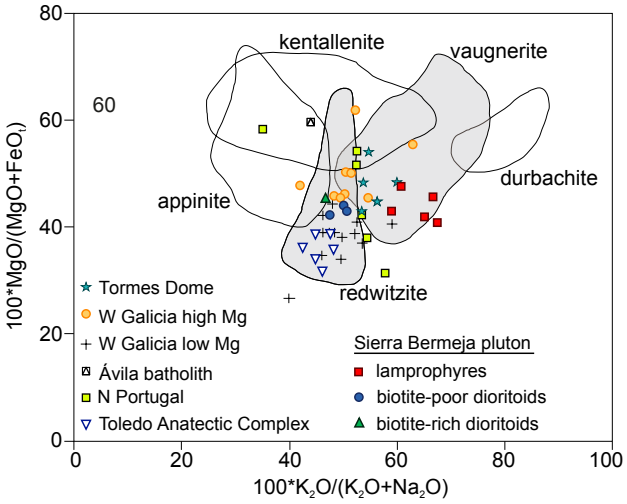

FIGURE 7. Projection of the vaugnerite series rocks of the Sierra Bermeja Pluton in the *mg* (100*MgO/[MgO+FeO$_t$]) *vs. k* (100*K$_2$O/[K$_2$O+Na$_2$O]) comparative diagram (Rock, 1991; Sabatier, 1991). Rock data compiled from Gil Ibarguchi (1981); Barbero *et al.* (1990); Barbero (1992); López Plaza *et al.* (1999); Dias *et al.* (2002); Gallastegui (2005) and Scarrow *et al.* (2009).

comprised between those of the high-Mg and low-Mg vaugnerites of western areas of Galicia and, in terms of *k* values, are also close to some samples of the Tormes Dome (Fig. 7). In conclusion, and according to the *mg vs. k* comparative diagram (Rock, 1991; Sabatier, 1991), the studied rocks of the Sierra Bermeja Pluton are to be classified correctly as redwitzites of the vaugnerites series, just like would be most equivalent rocks found in the Iberian Massif, showing *mg* and k ratios close to those of the redwitzites of western areas of Galicia (Gallastegui, 2005) and the vaugnerites *s.s.* of the Tormes Dome (López Plaza *et al.*, 1999).

Though the absence of whole-rock isotope (Sr, Sm-Nd) data precludes a precise assignment, the classification of the rocks studied as of vaugnerite series and calc-alkaline lamprophyres points to a probable provenance from a heterogeneous metasomatised mantle source, as it is generally accepted for similar rocks elsewhere (*e.g.* Turpin *et al.*, 1988; Rock, 1991; Holub, 1997; Janoušek and Holub, 2007; Solgadi *et al.*, 2007; Scarrow *et al.*, 2009; von Raumer *et al.*, 2014; Couzinié *et al.*, 2016).

Timing of vaugnerites and lamprophyres emplacement

Vaugneritic rocks in the Iberian Massif appear most often in spatial relation with Variscan syn- to late/post-collisional peraluminous granitoids, including anatectic sub-autochtonous granites in thermal dome areas to elongated granodiorite massifs. Within central sectors of the Central Iberian Zone, vaugnerites of La Calzadilla Pluton in the Tormes Dome were emplaced at *ca.* 318Ma (López-Moro *et al.*, 2017). Though coeval mantle and crustal melting in this area might have taken place at that time, heating effects on crustal rocks by mantle-derived melts seem negligible (López-Moro *et al.*, 2017). To the South, in the Ávila Batholith, the emplacement of mafic and ultramafic rocks has been dated at *ca.* 312Ma (Montero *et al.*, 2004), being regarded as coeval with the granitoids generation. Nevertheless, this age is markedly later than the maximum of crustal melting there, discarding again the involvement of mantle-derived melts in the crustal heating (Scarrow *et al.*, 2009). Furthermore, alkaline lamprophyres intruding into this batholith clearly post-date the emplacement of the host granitoids (Scarrow *et al.*, 2006, 2011; Orejana *et al.*, 2008). Finally, more to the South, in the Toledo Anatectic Complex, vaugnerites dated at *ca.* 308Ma (Bea *et al.*, 2006) provide relative young emplacement ages respect to the host migmatites.

Dioritoids and lamprophyres studied of the Sierra Bermeja Pluton in southern Central Iberian Zone crop out separately each other and define N20–40E-trending longitudinal mappable discrete bodies, parallel to one of the main cooling joint systems of this massif (Sarrionandia *et al.*, 2004). As previously stated, these rocks cross-cut the contacts between the different monzogranitic units of this pluton (Fig. 1C). At a first glance, cartographic relations suggest that the emplacement of the intermediate melts would be markedly later respect to that of peraluminous monzogranitic magmas, constituting two unrelated magmatic events. Nevertheless, vaugnerite series rocks and lamprophyres are exclusively confined within the limits of this monzogranitic massif, pointing undoubtedly to a constricted timing between the respective magmatic pulses. In this sense, the granitic peraluminous magmatism of the Nisa-Alburquerque-Los Pedroches Magmatic Alignment where the Sierra Bermeja Pluton is included is constrained in the interval 314–304Ma (García de Madinabeitia *et al.*, 2003; Carracedo *et al.*, 2009; Solá *et al.*, 2009; Gutiérrez-Alonso *et al.*, 2011). Hence, the emplacement of the three igneous units that constitute the Sierra Bermeja Pluton would be probably comprised in this age interval. Such assumed emplacement age interval for monzogranites, dioritoids and lamprophyres at Sierra Bermeja matches the zircon age-range of *ca.* 319–308Ma for vaugnerites *s.l.* elsewhere within the Iberian Massif (Montero *et al.*, 2004; Bea *et al.*, 2006; Rodríguez *et al.*, 2007; López-Moro *et al.*, 2017) and, furthermore, argues for almost contemporary mantle and crustal melting in southern areas of the Massif.

Textural and structural differences between dioritoids and lamprophyres attest to the existence of at least two independent mantle-derived magma pulses in the studied area. On the other hand, thought the marked linear trend

at map scale of the vaugnerites series bodies, at the outcrop they show sinuous or irregular trends standing out the absence of chilled margins at their edges and thermal effects in the host monzogranites. Moreover, the vaugneritic dioritoids are medium-grained rocks, which suggests that vaugneritic bodies were emplaced into the monzogranites with relatively low temperature contrast between them and, thus, probably before the complete consolidation of the monzogranites. In addition, the necking of the alignments and their dismembered terminations showing dispersed alineated enclaves points to a disruption of the vaugneritic intrusives suggesting that they would constitute syn-plutonic mafic dykes (*e.g.* Pitcher, 1997). The mixing/mingling textures described in the Petrography section are regarded as evidence of hybridisation of the intermediate magmas with a felsic magma, although the textural and modal characteristics of the observed felsic globules in the dioritoids discard their monzogranitic nature and hence limited contamination.

By contrast, lamprophyres show marked rectilinear trends and aphanitic textures at the field scale, which suggest brittle fracturing of monzogranites and higher temperature contrast during their emplacement. Moreover, the monzogranite enclaves found within the lamprophyres (Fig. 2C) show thermal (hydrothermal) effects on biotite and feldspars (Fig. 4D). These characteristics evidence that monzogranites were well highly consolidated and cool during the emplacement of lamprophyres.

The identification of vaugneritic dioritoids and calc-alkaline lamprophyres in southern areas of the Central Iberian Zone proves that mantle melting was a generalized process in the Iberian Massif during late- to post-Variscan stages. The emplacement of the vaugneritic rocks was almost contemporary with the generation of peraluminous granitic melts. The lamprophyric magmatism could probably represent the final stage of the late-Variscan events, constituting the marker of a new geodynamic regime (*e.g.* Scarrow *et al.*, 2011), clearly differentitated from the previous crustal melting processes.

CONCLUSIONS

Several NE–SW trending longitudinal bodies of mesocratic intermediate rocks have been identified within the cordierite-bearing monzogranites of the Sierra Bermeja Pluton (southern Iberian Massif). These intermediate rocks are i) dioritoid members of the vaugnerite series and ii) calc-alkaline lamprophyres. These rocks would constitute two independent mantle-derived magma pulses, a first one of vaugneritic type, which formed syn-plutonic dykes, and a later one of calc-alkaline lamprophyres that were emplaced after almost complete consolidation of the host monzogranites. Vaugneritic syn-plutonic dykes would represent the testimony of coeval mantle- and crustal-melting processes during a late-Variscan stage, while calc-alkaline lamprophyres would mark the ending of this stage.

ACKNOWLEDGMENTS

This work has been supported financially by the Spanish Ministerio de Ciencia e Innovación (MINECO, grant CGL2015-63530-P) and the University of the Basque Country (UPV/EHU, Grupo Consolidado project GIU15/05). The Geochronology and Isotope Geochemistry-SGIker facility (UPV/EHU, MINECO, GV/EJ, ERDF and ESF) and F. de la Cruz (UPV/EHU) are gratefully acknowledged, as well as M.A. Fernández from the University of Oviedo. J. Errandonea-Martin would also like to thank the grant from the UPV/EHU 2014 program. Finally, we appreciate the constructive comments of Jane H. Scarrow and Simone Tommasini, which have improved considerably the manuscript.

REFERENCES

Alonso Olazabal, A., 1999. Petrology, magnetic fabric and emplacement in a strike-slip regime of a zoned peraluminous granite: the Campanario-La Haba pluton, Spain. In: Castro, A., Fernández, C., Vigneresse, J.L. (eds.). Understanding Granites: Integrating New and Classical Techniques. London, Geological Society, 177-190. https://doi.org/10.1144/GSL.SP.1999.168.01.12

Alonso Olazabal, A., 2001. El plutón de Campanario-La Haba: caracterización petrológica y fábrica magnéti*ca*. PhD Thesis. University of the Basque Country, 323pp.

Barbero, L., 1992. Tres tipos de rocas gabroideas en el complejo de Toledo. Cadernos do Laboratorio Xeolóxico de Laxe, 17, 173-186.

Barbero, L., Villaseca, C., Andonaegui, P., 1990. On the origin of the gabbro-tonalite-monzogranite association from Toledo area (Hercynian Iberian Belt). Schweizerische Mineralogische und Petrografische Mitterlung, 70(2), 207-219. http://doi.org/10.5169/seals-53614

Bea, F., 2004. La naturaleza del magmatismo de la Zona Centro Ibérica: consideraciones generales y ensayo de correlación. In: Vera, J.A. (ed.). Geología de España. Madrid, Sociedad Geológica de España-Instituto Geológico y Minero de España (SGE-IGME), 128-133.

Bea, F., Montero, P., Molina, J.F., 1999. Mafic Precursors, Peraluminous Granitoids, and Late Lamprophyres in the Ávila Batholith: A Model for the Generation of Variscan Batholiths in Iberia. The Journal of Geology, 107(4), 399-419. https://doi.org/10.1086/314356

Bea, F., Montero, P.G., Gonzalez-Lodeiro, F., Talavera, C., Molina, J.F., Scarrow, J.H., Whitehouse, M.J., Zinger, T., 2006. Zircon thermometry and U–Pb ion-microprobe dating of the gabbros and associated migmatites of the Variscan Toledo Anatectic Complex, Central Iberia. Journal of the Geological Society, 163, 847-855. https://doi.org/10.1144/0016-76492005-143

Buda, G., Dobosi, G., 2004. Lamprophyre-derived high-K mafic enclaves in Variscan granitoids from the Mecsek Mts. (South Hungary). Neues Jahrbuch für Mineralogie-Abhandlungen: Journal of Mineralogy and Geochemistry, 180(2), 115-147. https://doi.org/10.1127/0077-7757/2004/0180-0115

Buzzi, L., Gaggero, L., Grozdanov, L.,Yanev, S., Slejko, F., 2010. High-Mg potassic rocks in the Balkan segment of the Variscan belt (Bulgaria): implications for the genesis of orogenic lamproite magmas. Geological Magazine, 147(3), 434-450. https://doi.org/10.1017/S0016756809990550

Carracedo, M., 1991. Contribución al estudio del batolito de Los Pedroches (Córdoba). PhD Thesis. University of the Basque Country, 443pp.

Carracedo, M., Paquette, J.L., Alonso Olazabal, A., Santos Zalduegui, J.F., García de Madinabeitia, S., Tiepolo, M., Gil Ibarguchi, J.I., 2009. U-Pb dating of granodiorite and granite units of the Los Pedroches batholith. Implications for geodynamic models of the southern Central Iberian Zone (Iberian Massif). International Journal of Earth Sciences, 98, 1609-1624. http://dx.doi.org/10.1007/s00531-008-0317-0

Carrington da Costa, J., 1950. Noticia sobre uma carta geologica do Buçaco, de Nery Delgado. Lisboa, Publicación Especial de la Comision de Servicio Geológico de Portugal, 1-27.

Castro, A., Patiño Douce, A.E., Corretgé, L.G., de la Rosa, J.D., El-Biad, M., El-Hmidi, H., 1999. Origin of peraluminous granites and granodiorites, Iberian massif, Spain: an experimental test of granite petrogenesis. Contributions to Mineralogy and Petrology, 135(2-3), 255-276. https://doi.org/10.1007/s004100050511

Castro, A., Corretgé, L.G., de la Rosa, J., Enrique, P., Martínez, F.J., Pascual, E., Lago, M., Arranz, E., Galé, C., Fernández, C., Donaire, T., López, S., 2002. Paleozoic magmatism. In: Gibbons, W., Moreno, T. (eds.). The Geology of Spain. London, Geological Society, 117-153.

Corretgé, L.G., Ugidos, J.M., Martínez, F.J., 1977. Les series granitiques varisques du secteur centre-occidental espagnol. La Chaine varisque d'Europe Moyenne et Occidentale. Colloque International, Centre National de la Recherche Scientifique, 243, 453-461.

Couzinié, S., Moyen, J.-F., Villaros, A., Paquette, J.-L., Scarrow, J.H., Marignac, C., 2014. Temporal relationships between Mg-K mafic magmatism and catastrophic melting of the Variscan crust in the southern part of Velay Complex (Massif Central, France). Journal of Geosciences, 59, 69-86. https://doi.org/10.3190/jgeosci.155

Couzinié, S., Laurent, O., Moyen, J.-F., Zeh, A., Vézinet, A., Villaros, A., 2015. Mg-K magmatic suites as a tool to scan the composition of the Variscan orogenic mantle, case studies from the French Massif Central. Geologié de la France, The Variscan belt: correlations and plate dynamics-Special meeting of the French & Spanish Geological Societies, 1, 43.

Couzinié, S., Laurent, O., Moyen, J.-F., Zeh, A., Bouilhol, P., Villaros, A., 2016. Post-collisional magmatism: Crustal growth not identified by zircon Hf–O isotopes. Earth and Planetary Science Letters, 456, 182–195. https://doi.org/10.1016/j.epsl.2016.09.033

Deer, W.A., Howie, R.A., Zussman, J., 1962. Rock-Forming Minerals. Vol. 3: Sheet Silicates. London, Longman. 270pp.

Deer, W.A., Howie, R.A., Zussman, J., 1963. Rock-Forming Minerals. Vol. 4: Framework Silicates. London, Longman. 435pp.

Del Olmo Sanz, A., Matia Villarino, G., Olivé Davó, A., Huerta Carmona, J., 1992. Hoja geológica número 752 (Mirandilla). Mapa Geológico de España a Escala 1:50.000. Madrid, Instituto Geológico y Minero de España (IGME). http://info.igme.es/cartografiadigital/geologica/Magna50Hoja.aspx?Id=752

Dias, G., Leterrier, J., 1994. The genesis of felsic-mafic plutonic associations: a Sr and Nd isotopic study of the Hercynian Braga Granitoid Massif (Northern Portugal). Lithos, 32(3-4), 207-223. https://doi.org/10.1016/0024-4937(94)90040-X

Dias, G., Simões, P.P., Ferreira, N., Leterrier, J., 2002. Mantle and Crustal Sources in the Genesis of Late-Hercynian Granitoids (NW Portugal): Geochemical and Sr-Nd Isotopic Constraints. Gondwana Research, 5(2), 287-305. https://doi.org/10.1016/S1342-937X(05)70724-3

Eguiluz, L., Apalategui, O., Carracedo, M., Sarrionandia, F., 2005. La zona de cizalla de Campillo: accidente tectónico a escala continental en el suroeste del Macizo Ibérico. Geogaceta, 37, 23-26.

Fournet, J., 1837. Geologie lyonnaise. Lyon, De Barret, 744pp.

Galán, G., Corretgé, L.G., Laurent, O., 1997. Low-potassium vaugnerites from Guéret (Massif Central, France). Mafic magma evolution influenced by contemporaneous granitoids. Mineralogy and Petrology, 59(3-4), 165-187. https://doi.org/10.1007/BF01161858

Gallastegui, G., 2005. Petrología del Macizo Granodiorítico de Bayo-Vigo (Provincia de Pontevedra, España). PhD Thesis. University of Oviedo, 414pp.

García de Madinabeitia, S., Santos Zalduegui, J.F., Gil Ibarguchi, J.I., Carracedo, M., 2003. Geocronología del plutón de Campanario-La Haba (Badajoz) a partir del análisis de isótopos de Pb en circones y U-Th-Pbtotal en monacitas. Geogaceta, 34, 27-30.

García de Madinabeitia, S., Sánchez Lorda, M.E., Gil Ibarguchi, J.I., 2008. Simultaneous determination of major to ultratrace elements in geological samples by fusion-dissolution and inductively coupled plasma mass spectrometry techniques. Analytica Chimica Acta, 625(2), 117-130. http://dx.doi.org/10.1016/j.aca.2008.07.024

Gil Ibarguchi, J.I., 1980. Las vaugneritas de la región de Finisterre (Galicia, NW. España). Probables productos de magmas anatécticos residuales. Cadernos do Laboratorio Xeolóxico de Laxe, 1, 21-32.

Gil Ibarguchi, J.I., 1981. A comparative study of vaugnerites and metabasic rocks from the Finisterre region (NW Spain). Neues Jahrbuch für Mineralogie–Abhandlungen, 143(1), 91-101.

Gil Ibarguchi, J.I., Bowden, P., Whitley, J.E., 1984. Rare Earth Element Distribution in Some Hercynian Granitoids from the Finisterre Region, NW Spain. The Journal of Geology, 92(4), 397-416. https://doi.org/10.1086/628875

González Menéndez, L., 1998. Petrología y geoquímica del batolito granítico de Nisa-Alburquerque (Alto Alentejo, Portugal; Extremadura, España). PhD Thesis. University of Granada, 221pp.

Gonzalo, J.C., 1987. Petrología y estructura del basamento hercínico del área de Mérida (Extremadura Central). PhD Thesis. University of Salamanca, 327pp.

Gutiérrez-Alonso, G., Fernández-Suárez, J., Jeffries, T.E., Johnston, S.T., Pastor-Galán, D., Murphy, J.B., Franco, M.P., Gonzalo, J.C., 2011. Diachronous post-orogenic magmatism within a developing orocline in Iberia, European Variscides. Tectonics, 30(5), TC5008. https://doi.org/10.1029/2010TC002845

Holub, F.V., 1997. Ultrapotassic plutonic rocks of the durbachite series in the Bohemian Massif: Petrology, geochemistry and petrogenetic interpretation. Sborník Geologických Věd, Ložisková Geologie-Mineralogie, 31, 5-26.

Irvine, T.N., Baragar, W.R.A., 1971. A guide to the chemical classification of the common volcanic rocks. Canadian Journal of Earth Sciences, 8(5), 523-548. https://doi.org/10.1139/e71-055

Janoušek, V., Holub, F.V., 2007. The causal link between HP-HT metamorphism and ultrapotassic magmatism in collisional orogens: case study from the Moldanubian Zone of the Bohemian Massif. Proceedings of the Geologists' Association, 118, 75-86. https://doi.org/10.1016/S0016-7878(07)80049-6

Janoušek, V., Rogers, G., Bowes, D.R., 1995. Sr-Nd isotopic constraints on the petrogénesis of the Central Bohemian Pluton, Czech Republic. Geologische Rundschau, 84(3), 520-534. https://doi.org/10.1007/BF00284518

Kováříková , P., Siebel, W., Jelínek, E., Štemprok, M., Kachlík, V., Holub, F.V., Blecha, V., 2007. Petrology, geochemistry and zircon age for redwitzite at Abertamy, NW Bohemian Massif (Czech Republic): tracing the mantle component in Late Variscan intrusions. Chemie der Erde-Geochemistry, 67(2), 151-174. https://doi.org/10.1016/j.chemer.2007.04.002

Kubínová, Š., Faryad, S.W., Verner, K., SchmitzM., Holub, F.V., 2017. Ultrapotassic dykes in the Moldanubian Zone and their significance for understanding of the post-collisional mantle dynamics during Variscan orogeny in the Bohemian Massif. Lithos, 272-273, 205-221. https://doi.org/10.1016/j.lithos.2016.12.007

Larrea, F.J., 1998. Caracterización petrológica y geoquímica del sector oriental del Batolito de Los Pedroches. PhD Thesis. University of the Basque Country, 459pp.

Laurent, O., Couzinié, S., Vanderhaeghe, O., Zeh, A., Moyen, J.-F., Villaros, A., Gardien V., 2015. U-Pb dating of Variscan igneous rocks from the eastern French Massif Central: southward migration of coeval crust- and mantle-melting witnesses late-orogenic slab retreat. Geologié de la France, The Variscan belt: correlations and plate dynamics-Special meeting of the French & Spanish Geological Societies, 1, 82.

Le Maitre, R.W., Streckeisen, A., Zanettin, B., Le Bas, M.J., Bonin, B., Bateman, P., Bellieni, G., Dudek, A., Efremova, S., Keller, J., Lameyre, J., Sabine, P.A., Schmid, R., Sorensen, H., Woolley, A.R., 2002. Igneous rocks: a classification and glossary of terms. Cambridge, Cambridge University Press, 236pp. https://doi.org/10.2113/gscanmin.40.6.1737

Leake, B.E., Woolley, A.R., Arps, C.E.S., Birch, W.D., Gilbert, M.C., Grice, J.D., Hawthorne, F.C., Kato, A., Kisch, H.J., Krivovichev, V.G., Linthout, K., Laird, J., Mandarino, J.A., Maresch, W.V., Nickel, E.H., Rock, N.M.S., Schumacher, J.C., Smith, D.C., Stephenson, N.C.N., Ungaretti, L., Whittaker, E.J.W., Guo, Y., 1997. Nomenclature of amphiboles: Report of the subcommittee on amphiboles of the International Mineralogical Association, Commission on New Minerals and Mineral Names. The Canadian Mineralogist, 35, 219-246.

López-Moro, F.-J., López-Plaza, M., 2004. Monzonitic series from the Variscan Tormes Dome (Central Iberian Zone): petrogenetic evolution from monzogabbro to granite magmas. Lithos, 72(1-2), 19-44. https://doi.org/10.1016/j.lithos.2003.08.002

López-Moro, F.-J., Romer, R.L., López-Plaza, M., González Sánchez, M., 2017. Zircon and allanite U-Pb ID-TIMS ages of vaugnerites from the Calzadilla pluton, Salamanca (Spain): dating mantle-derived magmatism and post-magmatic subsolidus overprint. Geologica Acta, 15(4), 395-408. http://dx.doi.org/10.1344/GeologicaActa2017.15.4.9

López Plaza, M., López Moro, F.J., Gonzalo Corral, J.C., Carnicero, A., 1999. Asociaciones de rocas plutónicas básicas e intermedias de afinidad calcoalcalina y shoshonítica y granitoides relacionados en el Domo Hercínico del Tormes (Salamanca y Zamora). Boletín de la Sociedad Española de Mineralogía, 22, 211-234.

López Sopena, F., Matia Villarino, G., del Olmo, A., Ortega Ruiz, I., 1990. Hoja geológica número 753 (Miajadas). Mapa Geológico de España a Escala 1:50.000. Madrid, Instituto Geológico y Minero de España (IGME). http://info.igme.es/cartografiadigital/geologica/Magna50Hoja.aspx?id=753

Michon, G., 1987. Les vaugnérites de l'Est du Massif central français: apport de l'analyse statistique multivariée à l'étude géochimique des éléments majeurs. Bulletin de la Société Géologique de France, 8, 591-600.

Middlemost, E.A.K., 1994. Naming materials in the magma/igneous rock system. Earth-Science Reviews, 37(3-4), 215-224. https://doi.org/10.1016/0012-8252(94)90029-9

Montel, J.M., 1988. First discovery of an orthopyroxene bearing vaugnerite: petrography, geochemistry, and implications on the genesis of vaugnerites. Comptes Rendus de l'Académie des Sciences de Paris, 306, 985-990.

Montel, J.M., Weisbrod, A., 1986. Charactéristiques and évolution of 'vaugnéritic magmas' an analytical and experimental approach, on the exemple of Cévennes Médianes (French Massif Central). Bulletin de Minéralogie, 109, 557-587.

Montero, P., Bea, F., Zinger, T.F., 2004. Edad 207Pb/206Pb en cristal único de circón de las rocas máficas y ultramáficas del sector de Gredos, Batolito de Ávila (Iberia Central). Revista de la Sociedad Geologica de España, 17, 157-165.

Morimoto, N., 1988. Nomenclature of Pyroxenes. Mineralogy and Petrology, 39(1), 55-76. https://doi.org/10.1007/BF01226262

Moyen, J.-F., Laurent, O., Chelle-Michou, C., Couzinié, S., Vanderhaeghe, O., Zeh, A., Villaros, A., Gardien, V., 2017. Lithos, 277, 154-177. https://doi.org/10.1016/j.lithos.2016.09.018

Orejana, D., Villaseca, C., Billström, K., Paterson, B.A., 2008. Petrogenesis of Permian alkaline lamprophyres and diabases from the Spanish Central System and their geodynamic context within western Europe. Contributions to Mineralogy and Petrology, 156, 477-500. https://doi.org/10.1007/s00410-008-0297-x

Palacios, T., Eguíluz, L., Apalategui, O., Jensen, S., Martínez-Torres, L.M., Carracedo, M., Gil Ibarguchi, J.-I., Sarrionandia, F., Martí, M., 2013. Mapa Geológico de Extremadura 1/350.000 y su memoria. Bilbao, Servicio Editorial de la UPV-EHU, 68x98cm, 222pp.

Pitcher, W.S., 1997. The nature and origin of granite. London, Springer Netherlands, 387pp. https://doi.org/10.1007/978-94-011-5832-9

Rock, N.M.S., 1991. Lamprophyres. Boston, MA, Springer US, 285pp. https://doi.org/10.1007/978-1-4757-0929-2

Rodríguez Alonso, M.D., Díez Balda, M.A., Perejón, A., Pieren, A., Liñan, E., López Díaz, F., Moreno, F., Gámez Vintaned, J.A., González Lodeiro, F., Martínez Poyatos, D., Vegas, R., 2004. La secuencia litoestratigráfica del Neoproterozoico-Cámbrico Inferior. In: Vera, J.A. (ed.). Geología de España. Madrid, Sociedad Geológica de España-Instituto Geológico y Minero de España (SGE-IGME), 78-81.

Rodríguez, J., Gil Ibarguchi, J.I., Paquette, J.L., 2007. Sincronía del magmatismo Varisco en el Macizo Ibérico: nuevas edades U-Pb en granitoides de la región de Finisterre (La Coruña, España). XV Semana – VI Congreso Ibérico de Geoquímica, Vila Real, Portugal, DVD-ROM (ISBN: 978-972-669-805-0), 146-149

Sabatier, H., 1980. Vaugérites et granites: une association particulière de roches grenues acides et basiques. Bulletin de Minéralogie, 103, 507-522.

Sabatier, H., 1991. Vaugnerites: special lamprophyre-derived mafic enclaves in some Hercynian granites from Western and Central Europe. In: Didier, J., Barbarin, B. (eds.). Enclaves and Granite Petrology. Developments in Petrology, Amsterdam, Elsevier, 63-81.

Sarrionandia, F., Carracedo, M., Eguíluz, L., Apalategui, O., 2004. Potencial ornamental del plutón de Sierra Bermeja (Badajoz): evaluación de su canterabilidad. Geogaceta, 35, 103-106.

Sauer, A., 1893. Der Granitit von Durbach im nordlichen Schwarzwald un seine Grenzfacies von Glimmersyenit (Durbachit). Mitteilung der Badischen Geologischen Landesanstalt, 2, 233-276.

Scarrow, J.H., Bea, F., Montero, P., Molina, J.F., Vaughan, A.P.M., 2006. A precise late Permian 40Ar/39Ar age for Central Iberian camptonitic lamprohyres. Geologica Acta, 4, 451-459. http://dx.doi.org/10.1344/105.000000346

Scarrow, J.H., Bea, F., Montero, P., Molina, J.F., 2008. Shoshonites, vaugnerites and potassic lamprophyres: similarities and differences between 'ultra'-high-K rocks. Earth and Environmental Science Transactions of the Royal Society of Edinburgh, 99, 159-175. https://doi.org/10.1017/S1755691009008032

Scarrow, J.H., Molina, J.F., Bea, F., Montero, P., 2009. Within-plate calc-alkaline rocks: Insights from alkaline mafic magma–peraluminous crustal melt hybrid appinites of the Central Iberian Variscan continental collision. Lithos, 110(1-4), 50-64. https://doi.org/10.1016/j.lithos.2008.12.007

Scarrow, J.H., Molina, J.F., Bea, F., Montero, P., Vaughan, A.P.M., 2011. Lamprophyre dikes as tectonic markers of late orogenic transtension timing and kinematics: A case study from the Central Iberian Zone. Tectonics, 30(4), TC4007. https://doi.org/10.1029/2010TC002755

Siebel, W., Chen, F., Satir, M., 2003. Late-Variscan magmatism revisited: New implications from Pb-evaporation zircon ages on the emplacement of redwitzites and granites in NE Bavaria. International Journal of Earth Sciences, 92(1), 36-53. https://doi.org/10.1007/s00531-002-0305-8

Solá, A.R., Williams, I.S., Neiva, A.M.R., Ribeiro, M.L., 2009. U-Th-Pb SHRIMP ages and oxygen isotope composition of zircon from two contrasting late Variscan granitoids, Nisa-Albuquerque batholith, SW Iberian Massif: Petrologic and regional implications. Lithos, 111(3-4), 156-167. http://dx.doi.org/10.1016/j.lithos.2009.03.045

Solgadi, F., Moyen, J.-F., Vanderhaeghe, O., Sawyer, E.W., Reisberg, L., 2007. The role of crustal anatexis and mantle-derived magmas in the genesis of synorogenic Hercynian granites of the Livradois Area, French Massif Central. The Canadian Mineralogist, 45, 581-606. http://dx.doi.org/10.2113/gscanmin.45.3.581

Sun, S.-S., McDonough, W.F., 1989. Chemical and isotopic systematics of oceanic basalts: implications for mantle composition and processes. In: Saunders, A.D., Norry, M.J., (eds.). Magmatism in the Ocean Basins. London, Geological Society, Special Publications, 42, 313-345. https://doi.org/10.1144/GSL.SP.1989.042.01.19

Turpin, L., Velde, D., Pinte, G., 1988. Geochemical comparison between minettes and kersantites from the Western European Hercynian orogen: trace element and Pb-Sr-Nd isotope constraints on their origin. Earth and Planetary Science Letters, 87, 73-86.

Villaseca, C., Barbero, L., Rogers, G., 1998. Crustal origin of Hercynian peraluminous granitic batholiths of Central Spain: petrological, geochemical and isotopic (Sr, Nd) constraints. Lithos, 43(2), 55-79. https://doi.org/10.1016/S0024-4937(98)00002-4

von Raumer, J.F., Finger, F., Veselá, P., Stampfli, G.M., 2014. Durbachites–Vaugnerites–a geodynamic marker in the central European Variscan orogen. Terra Nova, 26(2), 85-95. https://doi.org/10.1111/ter.12071

Willmann, K., 1920. Die Redwitzite, eine neue Gruppe von granitischen Lamprophyren. Zeitschrift der Deutschen Geologischen Gesellschaft, 71, 1-33.

Manuscript received September 2017;
revision accepted March 2018;
published Online June 2018.